Hindawi
Science and Technology of Nuclear Installations
Volume 2023, Article ID 7402217, 12 pages
https://doi.org/10.1155/2023/7402217

Research Article

Accident Sequence Precursor Analysis of an Incident in a Japanese Nuclear Power Plant Based on Dynamic Probabilistic Risk Assessment

Kotaro Kubo

Nuclear Safety Research Center, Japan Atomic Energy Agency, 2-4 Shirakata, Tokai-Mura, Naka-Gun, Ibaraki 319-1195, Japan

Correspondence should be addressed to Kotaro Kubo; kubo.kotaro@jaea.go.jp

Received 19 December 2022; Revised 13 March 2023; Accepted 20 March 2023; Published 7 June 2023

Academic Editor: Keith E. Holbert

Probabilistic risk assessment (PRA) is an effective methodology that could be used to improve the safety of nuclear power plants in a reasonable manner. Dynamic PRA, as an advanced PRA, allows for more realistic and detailed analyses by handling time-dependent information. However, the applications of this method to practical problems are limited because it remains in the research and development stage. This study aimed to investigate the possibility of utilizing dynamic PRA in risk-informeddecision-making. Specifically, the author performed an accident sequence precursor (ASP) analysis on the failure of emergency diesel generators that occurred at Unit 1 of the Tomari Nuclear Power Plant in Japan using dynamic PRA. The results were evaluated by comparison with the results of simplified classical PRA. The findings indicated that dynamic PRA may estimate lower risks compared with those obtained from classical PRA by reasonable modeling of alternating current power recovery. The author also showed that dynamic PRA can provide detailed information that cannot be obtained with classical PRA, such as uncertainty distribution of core damage timing and importance measure considering the system failure timing.

1. Introduction

Probabilistic risk assessment (PRA) is a very useful, well-developed method to understand risk in complex systems such as nuclear power plants. Many countries have used this type of assessment for risk-informeddecision-making (RIDM). For example, in the U.S., the Nuclear Regulatory Commission (NRC) uses PRA in their significance determination process (SDP) [1], Mitigating Systems Performance Index (MSPI) [2], and Management Directive 8.3 (MD 8.3) [3] as components of the reactor oversight process (ROP) [4]. PRA is also used to extend the individual allowed outage time (AOT)/completion time (CT) (Initiative 4A) [5], risk-informed CT (Initiative 4B) [6], and Surveillance Frequency Control Program (Initiative 5B) [7]. The NRC finds that "PRA methods, models, tools, and data are sufficiently mature to support risk-informed decision making at the NRC" [8]. In Japan, the Nuclear Regulation Authority (NRA) uses PRA for regulatory inspection, referencing the NRC's ROP [9].

One of the limitations of this method, however, is the difficulty of modeling temporal information. Specifically, temporal distributions of system failure timing, core damage timing, and recovery timing are difficult to assess the explicitly in classical PRA. Several dynamic PRA methods and tools have been developed and applied to some safety issues to overcome this difficulty. Verma et al. classified dynamic PRA methods into six methods, namely, Monte Carlo simulation, continuous event trees, discrete dynamic event trees (DDET), dynamic flow graph methodology, Markov modeling/Petri nets, and dynamic fault trees [10]. For example, RAVEN (reactor analysis and virtual control environment) has Monte Carlo-based sampler and many types of algorithms for dynamic PRA, optimization, data mining, and the like [11, 12]. ADS-IDAC (accident dynamic simulator coupled with the information, decision, and action in a crew context) is a tool based on DDET and featuring an advanced human reliability model [13, 14]. MCDET (Monte Carlo dynamic event tree) enables the proper use of the

Monte Carlo method and DDET [15, 16]. Tools such as ADAPT (analysis of dynamic accident progression trees) [17, 18], SCAIS (simulation code system for integrated safety assessment) [19, 20], PyCATSOO (Pythonic object-oriented hybrid stochastic automata) [21, 22], DICE (dynamic integrated consequence evaluation) [23, 24], MOSAIQUE (module for sampling input and quantifying estimator) [25, 26] have also been developed.

The Japan Atomic Energy Agency (JAEA) has been developing the dynamic PRA methodology. This method enables analysts to obtain more realistic and detailed results compared with those produced by classical PRA by processing the time-related information via coupling probabilistic sampling and thermal–hydraulics (T–H) simulation, as shown in Figure 1. In this methodology, not only system failure probabilities but also failure timing can be handled explicitly. To realize this method, the author used RAPID (risk assessment with plant interactive dynamics) framework [27–29] and THALES-2 (thermal hydraulic analysis of loss of coolant, emergency core cooling, and severe core damage, version 2) T–H analysis code [30–34]. Risk assessments of the randomly- and seismically-induced internal flooding were conducted using these codes [35, 36].

However, unlike classical PRA, only a few cases of the use of dynamic PRA in RIDM have been reported. More case studies need to be performed to investigate the applicability of dynamic PRA for RIDM, including accident sequence precursor (ASP) analysis. ASP is performed by regulatory agencies to evaluate the potential of core damage based on operating experiences. Therefore, the author selected it as a representative of RIDM. The procedure of ASP is described in Section 4.6.

In this paper, the dynamic PRA-based ASP of a Japanese nuclear power plant incident was performed with reference to the results of the literature review of representative dynamic PRA-based ASP. The advantages of dynamic PRA in ASP were extracted by comparing the results with those of classical PRA. Furthermore, risk information obtained by dynamic PRA that cannot be obtained by classical PRA was presented.

2. Literature Review of ASP Analysis Using Dynamic PRA

This section summarizes the information obtained from a literature review on two dynamic PRA-based ASP analyses.

2.1. ASP Analysis of Loss of a Reactor Coolant Pump Seal Cooling Event. Coyne et al. performed a case study on ASP analysis using dynamic PRA [37]; here, the selected event was the loss of reactor coolant pump (RCP) seal cooling induced by an electrical fire at the Robinson nuclear power plant on March 28, 2010 [38]. The analysis was performed using RELAP (reactor excursion and leak analysis program) [39] and ADS-IDAC [13].

In their analysis, the authors focused on the rate of leakage from the RCP seal. This rate is a critical parameter describing the scale of loss of coolant accident (LOCA) model in classical PRA. In standardized plant analysis risk (SPAR) models [40] based on the classical PRA model developed by the U.S. NRC, two leakage rates (4.8 m^3/h (21 gallons per minute (gpm)) per pump and 109 m^3/h (480 gpm) per pump) were modeled to simulate small and medium LOCAs. Specific risk value was not quantified in the author's analysis. However, the results reported by them showed that the most conservative leakage rate of 480 gpm was demonstrated to likely behave like a small LOCA. Thus, the authors argued that dynamic PRA could improve communication with decision-makers by clearly demonstrating the impact of high-risk scenarios compared with classical PRA.

2.2. ASP Analysis of a Steam Generator Tube Rupture Event. Lee et al. performed dynamic PRA-based ASP analysis of a steam generator tube rupture (SGTR) that occurred at the Ulchin nuclear power plant in Korea on April 5, 2002 [41]. Information on this incident is available in OPIS (operational performance information system for nuclear power plant), which is managed by the Korea Institute of Nuclear Safety (KINS) [42]. The MARS (multidimensional analysis of reactor safety) [43] and MOSAIQUE [25] were used to quantify the total conditional core damage probability (CCDP).

The results of classical and dynamic PRA were compared, and the total CCDP obtained by classical PRA was in the order of 10^{-3}. By comparison, the total CCDP determined by dynamic PRA was in the order of 10^{-4}. The group thus concluded that dynamic PRA could quantify risk using a best-estimate approach and eliminate the conservatism featured in classical PRA. Specifically, the realistic handling of shutdown mode and operator action enables to obtain lower calculated CCDP.

3. Selected Japanese Incident

An incident that occurred at Unit 1 of the Tomari Nuclear Power Plant in Japan in September 2007 was selected. In this incident, two emergency diesel generators (EDGs) became unavailable within a short period. At the time of this incident, the plant was in full-power operation mode and eventually shut down by the operator. The simplified scenario of this incident is summarized in Figure 2. The above information is available in the Japanese nuclear power plant incident database, called NUCIA (nuclear information archives) [44] and a report published by the Japan Nuclear Energy Safety Organization (JNES) [45]. Note that the reactor trip means inserting the control rods and that the shutdown means stopping the electric power generation.

As shown in Figure 2, the status of each EDG, which was estimated from the timeline described above, may be available, degraded, or unavailable. The status of each EDG can also be classified into six states.

Prior to August 21, 13 : 37, the EDGs could be assumed to be available (base state). Because EDG-B failed to start during the surveillance test on September 18, the system could be inferred to be degraded in the period between

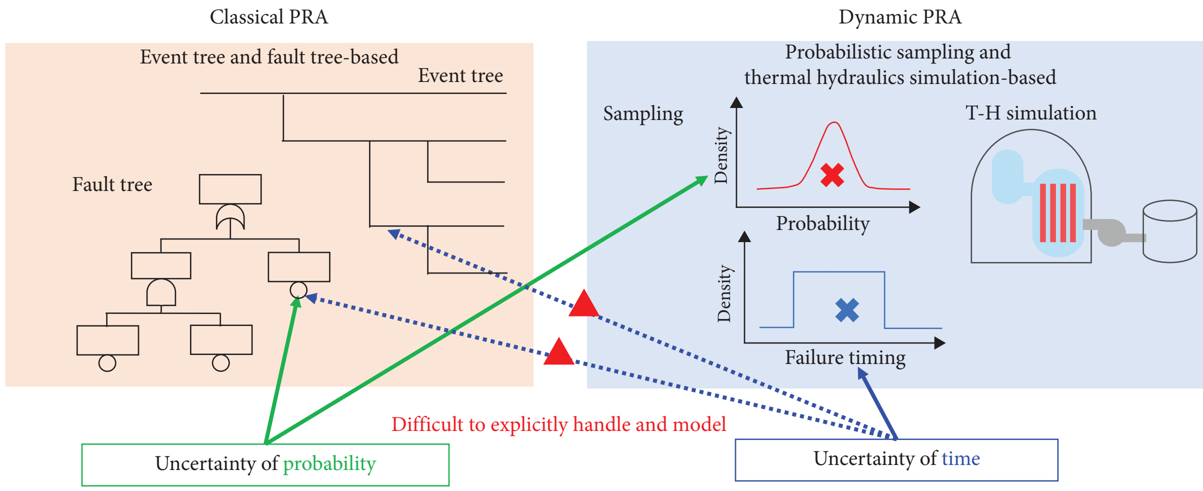

Figure 1: Classical PRA and dynamic PRA.

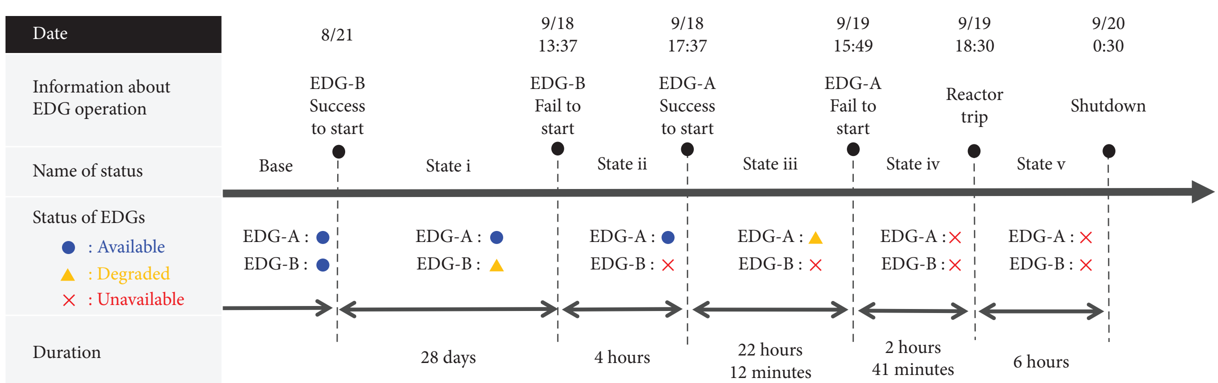

Figure 2: Summary of Unit 1 of the Tomari nuclear power plant incident.

August 21 and September 18 (State i). Then, after 4 h, EDG-A was successfully started. Therefore, EDG-A was determined to be available up to 17 : 37 (State ii). When the status check of EDG-A was done at 15 : 49 on September 19, the generator failed to start to run. Thus, the author defined the period before this time as State iii and the period 2 h from this time to the reactor trip as State iv. After 6 h, electric power generation ceased. The period from the reactor trip to the cessation of electric generation was defined as State v.

4. Analytical Methodology

This section describes the accident scenario, analysis codes, and probabilistic models used to evaluate the risk of a selected event.

4.1. Accident Scenarios. To model the incident mentioned above, the author assumed that the dominant initiating event causing core damage was the loss of offsite power (LOOP). Therefore, in this study, LOOP-initiated accident scenarios, including station blackout (SBO), were evaluated.

Figure 3 shows the simplified event tree of LOOP. The author assumed that the frequency of LOOP is 1×10^{-2}/reactor year and that the reactor trip would always be successful upon the occurrence of LOOP. When both EDG-A and EDG-B fail, the plant experiences SBO. In the early phase of the SBO, the turbine-driven auxiliary feedwater systems (AFWs) are available, but they become unavailable in the late phase. This unavailability is caused by the depletion of the direct current (DC)-power supply from the battery, thus rendering the operation of the air-operated valve necessary to adjust the steam flow rate to drive AFWs impossible.

For the recovery action, the author modeled alternating current (AC)-power recovery and its timing following a normal distribution with a mean value (μ) and standard deviation (σ) of 8.0 and 2.0 h, respectively. This recovery makes the AFWs and high-pressure injection systems (HPIs) available, thus injecting water from the condensate storage tank (CST) to the secondary side of steam generator (SG) and the refueling water storage tank (RWST) to reactor vessel (RV). Note that Japanese nuclear power plants have their own alternate AC-power sources after the Fukushima Daiichi Nuclear Power Plant accident as a measure against SBO [46, 47]. Therefore, AC-power recovery time is plant-specific value, and although a hypothetical probability

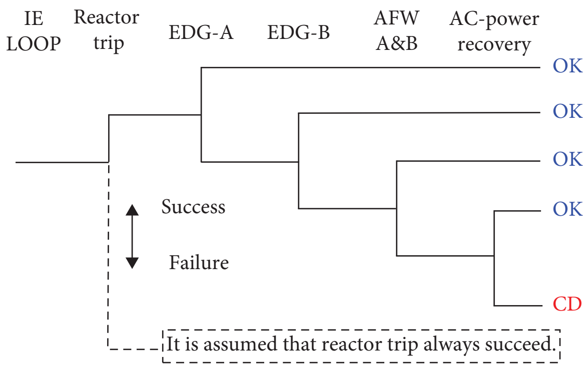

FIGURE 3: Event tree.

distribution is set in this study, it is obtained by detailed engineering judgment.

4.2. Probabilistic Modeling of EDG Failure. In this study, the failure probability and timing were assumed, as shown in Table 1. In classical PRA, two types of failure models are generally used [48]: the time-related failure model and the demand model.

Time-related failures are generally modeled using the exponential failure density function given in equation (1) under the assumption that the failure rate remains constant over time.

$$f(t) = \lambda \exp^{-\lambda t}, \tag{1}$$

where λ is the failure rate (/unit time) and t is the time. The time-related failure probability is obtained by integrating equations (1) with time and presented in (2).

$$p(t) = 1 - \exp^{-\lambda t}. \tag{2}$$

The binomial distribution is generally used for the demand failure model. In this study, evaluation was conducted under the assumption that time-related failures are dominant. In this failure mode, as shown in equation (2), a mission time is required to calculate the failure probability. In general, 24 h is used as the mission time in classical PRA. However, the validity of applying this mission time to dynamic PRA has not been sufficiently verified. Thus, the author did not integrate the failure rate with time and set the failure probability at the base state to 1×10^{-2}. For failure timing, the author assumed a uniform distribution in the range of 0–4 h.

For State i, the author set the failure probability of EDG-B to 10 times higher than the base state because of the degradation of EDG-B. For failure timing, the uniform distribution in the range of 0–4 h is identical to that in the base state. For State ii, the failure probability of EDG-B was set to 1 because of the failure of EDG-B. The failure timing was assumed to have a normal distribution with μ and σ of 1.0 and 0.1 h, respectively. For State iii, besides the failure of the EDG-B, the degradation of EDG-A was considered, and the failure probability of EDG-A was set to 10 times the base state. For State iv, the failure probability of EDG-A was set to 1 because of the failure of the EDG-A. The failure timing was assumed to have a normal distribution with μ and σ of 1.0 and 0.1 h, respectively. The author excluded State v from the evaluation because it is not subject to the PRA at power, but for the PRA at low power or shutdown mode.

4.3. Probabilistic Modeling of AFW Failure. AFWs are turbine-driven and available only in the early phase of SBO. Therefore, the AFWs were modeled as a follow-on failure after the failure of EDG-A and EDG-B. The interval between the failure of the EDGs and AFWs was determined by the depletion time of the DC-power supply from the battery, which was assumed to follow a normal distribution with μ and σ of 4.0 and 1.0 h, respectively. If either EDG was available, i.e., SBO did not occur, only the random failure of the AFWs was considered. The failure probability was set to 1×10^{-2} and the failure timing was set to a normal distribution with μ and σ of 12.0 and 3.0 h, respectively.

4.4. Dynamic PRA Approach. THALES-2 and RAPID were coupled to perform dynamic PRA; here, RAPID provided the failure probability and timing described in Sections 4.1 to 4.3 for THALES-2. The core damage criterion was set when the peak cladding temperature (PCT) exceeded 1200°C, referring to the Japanese PRA standard [49]. Figure 4 shows a schematic of the system, where the abbreviations used are defined in the acronyms section.

4.5. Classical PRA Approach. The author used SAPHIRE (system analysis programs for hands-on integrated reliability evaluations) code [50] to execute the classical PRA approach. The fault tree of the mitigation systems is shown in Figure 5. Failure probabilities were modeled against the basic events in this fault tree. Note that the failure timings were ignored in this approach.

The minimal cut set (MCS) of this fault tree is represented by equation (3). The dynamic handling of the failure probabilities in this equation is limited. However, it is possible to quantify the occurrence probability of a top event at a given point in time, i.e., the probability of failure of the mitigation system or core damage.

$$\begin{aligned} \mathrm{MCS} = {} & \mathrm{EDG}_A \times \mathrm{EDG}_B + \mathrm{EDG}_A \times \mathrm{AFW}_B \\ & + \mathrm{AFW}_A \times \mathrm{EDG}_B + \mathrm{AFW}_A \times \mathrm{AFW}_B. \end{aligned} \tag{3}$$

The failure probability of AC-power recovery depends on the failure timing of the EDGs, AFWs, the decay heat generated in the reactor core, and their uncertainty. Thus, determining a unique value in classical PRA is challenging. This recovery is modeled by providing the heading in the event tree and/or reducing the failure probability of the basic event, in addition to engineering judgment. This study modeled the failure probability of AC-power recovery (P_{AC-rec}) as the event tree's heading, as shown in Figure 3. The value assigned to this probability was determined based on the relationship between the time margin (t_m) required to avoid core damage and the cumulative distribution function of the AC-power recovery

Table 1: Assumed reliability model of EDGs.

Status	EDG-A		EDG-B		Remark
	Failure probability (–)	Failure timing (h)	Failure probability (–)	Failure timing (h)	
Base	1×10^{-2}	Uniform (0, 4)	1×10^{-2}	Uniform (0, 4)	Assuming normal condition
State i	1×10^{-2}	Uniform (0, 4)	1×10^{-1}	Uniform (0, 4)	Assuming degradation of EDG-B, set failure rate 10 times higher than the base case
State ii	1×10^{-2}	Uniform (0, 4)	1	Normal (1, 0.1)	EDG-B failure is assumed to occur with certainty, and the time of occurrence is assumed to be uncertain
State iii	1×10^{-1}	Uniform (0, 4)	1	Normal (1, 0.1)	Assuming degradation of EDG-A, set failure rate 10 times higher than the base case
State iv	1	Normal (1, 0.1)	1	Normal (1, 0.1)	EDG-A failure is assumed to occur with certainty, and the time of occurrence is assumed to be uncertain
State v	—				This state is in scope of low-power or shutdown mode PRA and excluded from our evaluation

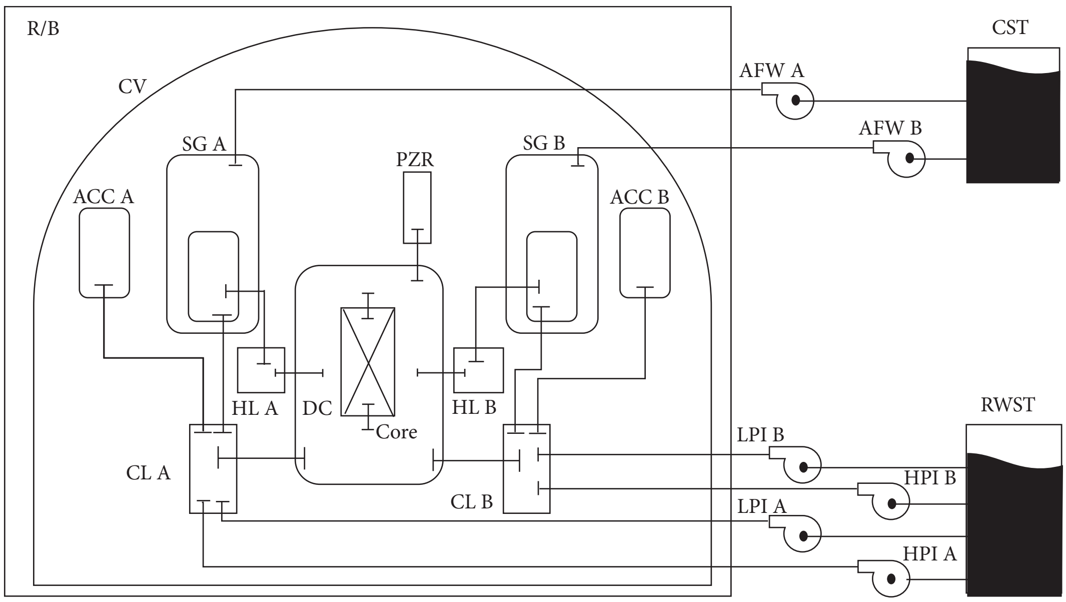

Figure 4: PWR modeling in THALES-2.

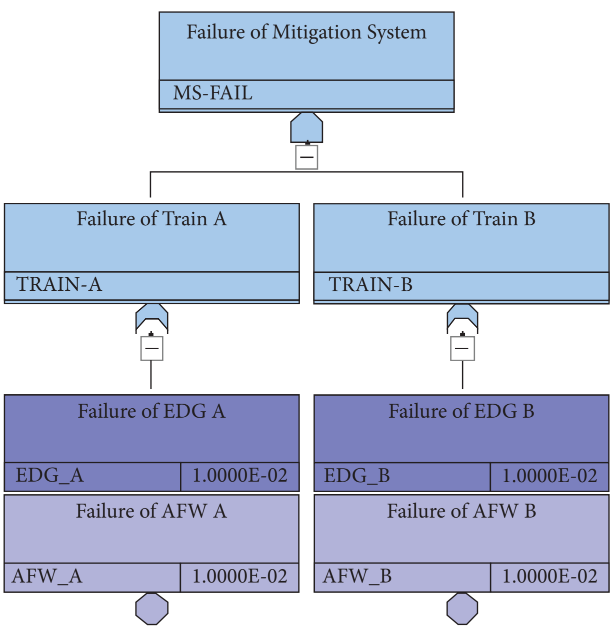

Figure 5: Fault tree of the mitigation systems.

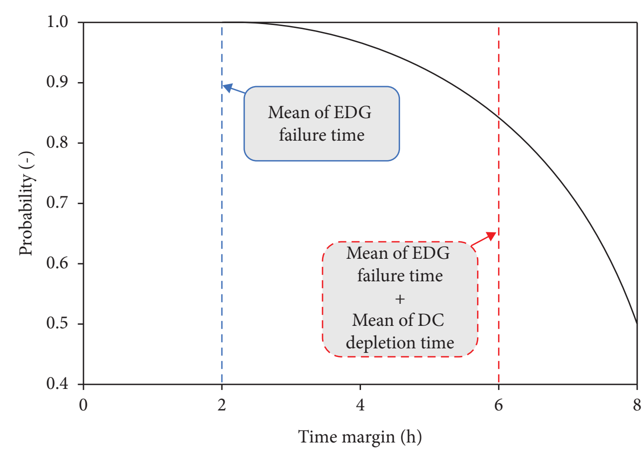

Figure 6: Sensitivity of the time margin to the failure probability of AC-power recovery.

time following a normal (8.0, 2.0) (equation (4)). Note that t_m represents the latest time by which AC-power must be recovered to prevent core damage.

$$P_{AC-rec} = 1.0 - \int_0^{t_m} \left\{ \frac{1}{\sqrt{2\pi\sigma^2}} \exp\left(-\frac{(x-\mu)^2}{2\sigma^2} \right) \right\} dx. \quad (4)$$

Figure 6 illustrates the sensitivity of the time margin to the failure probability of AC-power recovery. For instance, if 2.0 h (the mean of the EDG failure time following uniform (0.0, 4.0)) is assumed, the failure probability is approximately 1. Assuming 6.0 h (the sum of the mean of the EDG failure time and the mean of depletion time of the DC-power source since the start of the SBO condition) results in a failure probability of 0.84. Although applying a longer time margin leads to lower calculated risk metrics, such as core damage frequency, it typically requires technical justification. In some cases, high-level simulations, equivalent to dynamic PRA, are necessary to demonstrate the relationship between decay heat and heat removal performance by the cooling systems, including treating their uncertainties. In this study, the time margin of 0.0 h was the condition without AC-power recovery. The time margin was 6.0 h with AC-power recovery, representing the time between the LOOP occurrence and the depletion of the DC-power source in the base state.

4.6. ASP Procedure. In the ASP, the incidents were divided into the following two groups [51]:

(i) Failure or deterioration of equipment without an initiating event

(ii) Initiating event only, or failure or deterioration of equipment with initiating event

The former is evaluated by the change of core damage probability (ΔCDP). The latter is evaluated by CCDP. The incident selected in this study corresponds to the former. The ΔCDP is defined by following equation.

$$\Delta \mathrm{CDP} = \sum_{i=1}^{4} \left[\left(\mathrm{CDF}_i - \mathrm{CDF}_{\mathrm{base}} \right) \times \Delta t_i \right], \quad (5)$$

where CDF_i is the core damage frequency under status i shown in Figure 2, $\mathrm{CDF}_{\mathrm{base}}$ is the core damage frequency under the base status, Δt_i is the exposure time of status i, and CDF_i of dynamic PRA is defined by following equation.

$$\mathrm{CDF}_i = \mathrm{CCDP}_i \times F_{\mathrm{IE}} = \frac{N_{\mathrm{CD},i}}{N_{\mathrm{Total},i}} \times F_{\mathrm{IE}}, \quad (6)$$

where CCDP_i is CCDP under status i, F_{IE} is the frequency of the initiating event, $N_{\mathrm{CD},i}$ is the number of simulations leading to core damage, and $N_{\mathrm{total},i}$ is the total number of simulations under status i.

The calculated ΔCDP was classified into four colors according to severity. The U.S. NRC's color-coding scheme is shown in Table 2.

Table 2: U.S. NRC's color-coding scheme [51].

Color	Result	Decision
Red	$10^{-4} \le \Delta\mathrm{CDP}$	High safety significance
Yellow	$10^{-5} \le \Delta\mathrm{CDP} < 10^{-4}$	Substantial safety significance
White	$10^{-6} \le \Delta\mathrm{CDP} < 10^{-5}$	Low to moderate safety significance
Green	$\Delta\mathrm{CDP} < 10^{-6}$	Very low safety significance

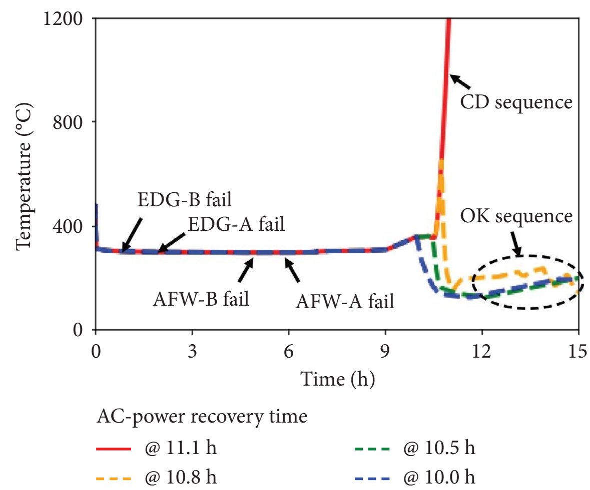

Figure 7: Example of PCT of the accident sequence.

5. Results and Discussion

5.1. Example of Plant Response Analyzed by THALES-2. Figure 7 shows the time variations of PCT with the accident scenarios shown in Table 3 as examples of reactor response. In this figure, the solid red line indicates core damage. Dashed lines avoid core damage by AC-power recovery. After the failure of EDG-A and EDG-B, PCT is maintained at approximately 300°C because of heat removal by AFWs. After the failure of AFWs, the steam generators dry out. PCT then begins to rise at approximately 10.5 h. If AC-power is recovered before 10.8 h, the reactor core could remain intact. The dynamic PRA can handle several uncertainties including system failure timing and AC-power recovery time and provide to the analyst realistic results.

Table 3: Event timing of the accident sequences shown in Figure 7.

Time (h)	Event	Remark
0.0	Occurrence of LOOP	—
1.0	EDG-B failure	Mean value of state iii
2.0	EDG-A failure	Mean value of state iii
5.0	AFW-B failure	Random failure did not occur
6.0	AFW-A failure	Random failure did not occur

5.2. Result of CDF Calculation and ASP Analysis. Table 4 shows the CDF of each PRA model. As the status progressed, CDF increased on account of severe conditions related to the reliability of the EDGs. Consideration of AC-power recovery using the dynamic PRA method lowered the CDF by approximately one order of magnitude. Similar to that of classical PRA shown in the second column, the CDF of dynamic PRA increased as the status progressed.

Figure 8 shows the ΔCDP of each case investigated in this work. The ΔCDP values of classical PRA (red) and dynamic PRA without AC-power recovery (orange) were of the same order of magnitude. This result means similar results can be expected if classical and dynamic PRA are modeled equivalently. However, the ΔCDP of classical PRA with AC-power recovery (green) and dynamic PRA with AC-power recovery (blue) differed by approximately one order of magnitude. This discrepancy is due to the difference in the modeling of AC-power recovery. Dynamic PRA could manage the uncertainty related to AC-power recovery more reasonably and realistically than classical PRA. Therefore, the results of dynamic PRA were observed to be lower than that of classical PRA.

A ΔCDP of 10^{-6} is assigned the color white and a ΔCDP of 10^{-7} is assigned the color green in the color scheme of the U.S. NRC. If the evaluation methods used to obtain color codes are more realistic, decision-makers may be able to make more rational decisions. In other words, effective regulations and safety improvement could be implemented. Therefore, it can be said that dynamic PRA can be a tool for rational decision-making.

Figure 9 shows the sensitivity analysis result of the time margin for AC-power recovery to the total ΔCDP calculated by classical PRA. The time margin should be approximately 10 h to reduce the total ΔCDP to 10^{-6}. This criterion is consistent with the typical T–H behavior shown in Figure 7. However, detailed simulations related to decay heat and

Table 4: CDF of classical and dynamic PRAs.

Status	Classical PRA		Dynamic PRA	
	Without AC-power recovery	With AC-power recovery	Without AC-power recovery	With AC-power recovery
Base	4.0×10^{-6}	3.4×10^{-6}	5.0×10^{-6}	6.0×10^{-8}
State i	1.8×10^{-5}	1.5×10^{-5}	3.2×10^{-5}	1.3×10^{-6}
State ii	2.2×10^{-4}	1.9×10^{-4}	2.4×10^{-4}	1.3×10^{-5}
State iii	1.1×10^{-3}	9.2×10^{-4}	1.1×10^{-3}	1.1×10^{-4}
State iv	1.0×10^{-2}	8.4×10^{-3}	1.0×10^{-2}	1.6×10^{-3}

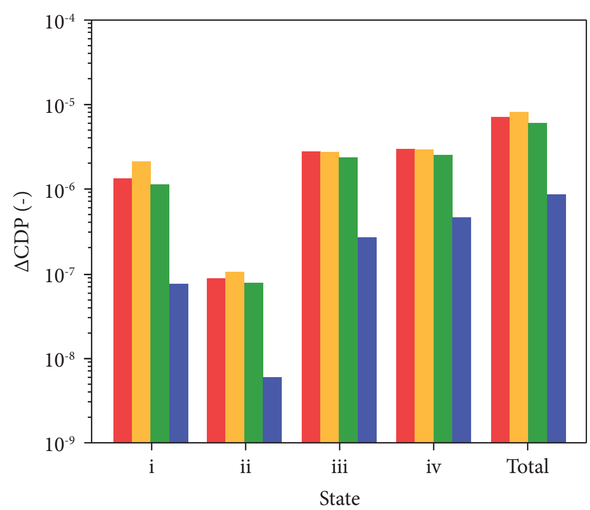

Figure 8: ΔCDP.

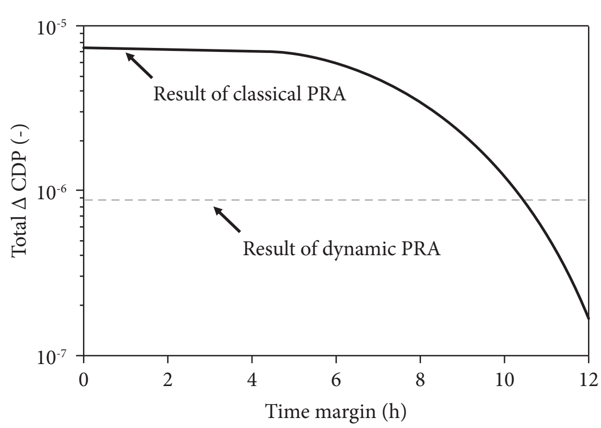

Figure 9: Sensitivity of the time margin to ΔCDP by classical PRA.

coolability via the mitigation system must be conducted to credit this criterion in classical PRA. In the dynamic PRA, a single value for the time margin need not be defined, as T–H simulations are performed for all accident scenarios. Furthermore, time-related uncertainty can be considered more realistic.

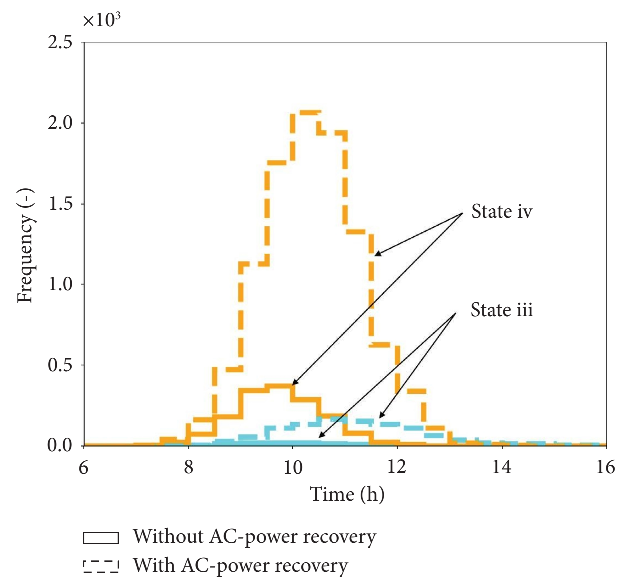

Figure 10: Histogram of core damage timing.

5.3. Risk Information Obtained by Dynamic PRA. Figure 10 shows a histogram of the core damage timing in States iii and iv. Focused on State iv, core damage occurred in the range 7–13 h and the mode is approximately 10.5 h. The magnitude of the histogram decreased and its peak shifted to the left as the AC-power was recovered. These results related to core damage timing including uncertainty cannot be obtained by classical PRA that evaluates only the presence or absence of core damage. This information is helpful for levels 2 and 3 PRA and evacuation planning because it can be used as an input value when examining the available time for measures to prevent damage of containment vessel and initiate evacuation.

Importance measure is a valuable information that can be obtained from PRA. Fussel–Vesely [52], risk reduction worth (RRW) [53], risk achievement worth (RAW) [53], Birnbaum [54], and differential importance measure (DIM) [55] were proposed in classical PRA. Several importance measures for dynamic PRA were suggested and applied [56–58]. The author introduced a new measure of time-dependent RAW (RAW_t), defined as equation (6), to discuss risk information obtained from dynamic PRA.

$$RAW_t = \frac{F(CD \mid A = 1, t = x)}{F(CD)}, \quad (7)$$

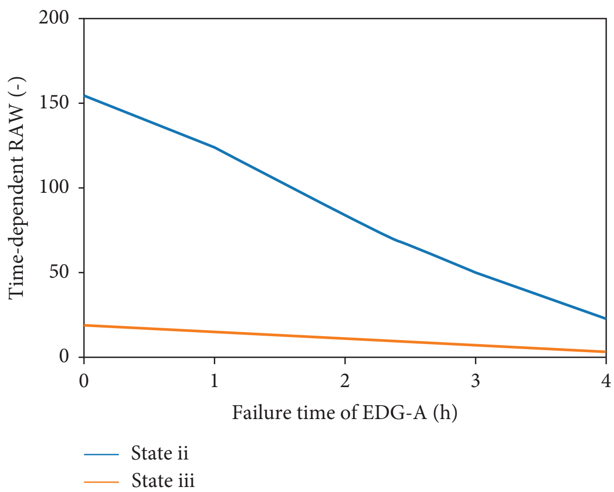

FIGURE 11: Time-dependent RAW of EDG-A.

where $F(\mathrm{CD})$ is CDF at nominal failure probability and its timing. $F(\mathrm{CD} \mid A = 1, t = x)$ is CDF with event A's probability set to 1 and its occurrence timing set to x.

Figure 11 shows the RAW_t values of EDG-A at States ii and iii with AC-power recovery. The RAW_t of State ii is approximately six times larger than that of State iii. The difference noted may be attributed to the denominator for State ii in equation (6) being smaller than that for State iii. This result indicates that the risk increases more in State ii than in State iii when EDG-A failure is assumed.

The RAW_t for State ii under the assumption that EDG-A would fail without working was approximately 150. Assuming that EDG-A fails after operating for 4 h, RAW_t was approximately 30. This difference indicates that if EDG-A fails after 4 h of operation, the increase in risk is about 1/5 of that when it fails without operation. This importance measure demonstrates that the amount of risk increase may be quantified in more detail than classical PRA by considering not only whether the system will fail or not but also when it will fail. Using the importance measure depending on the time obtained by dynamic PRA could help to improve the reliability of mitigation systems and to prevent increasing core damage risk efficiently. In addition, such time-dependent importance measure can be a reference for the perspective to be checked in case of an actual incident or accident.

6. Conclusions

This paper performed an ASP analysis of a Japanese nuclear power plant incident using dynamic and classical PRAs with some assumptions and simplifications. The ΔCDP values of these PRAs were of the same order of magnitude under the equalized condition, i.e., ignoring AC-power recovery. However, under the condition where AC-power recovery was considered, the ΔCDP of dynamic PRA was approximately one order of magnitude lower than that of classical PRA because the time-dependent uncertainty of AC-power recovery could be modeled reasonably. These results support the proposal of Lee et al. [41] that the risk calculated by dynamic PRA is lower than that obtained by classical PRA when using a best-estimate approach.

The sensitivity analysis of the time margin of AC-power recovery for avoiding core damage in classical PRA was performed, and the resulting total ΔCDP was investigated. A time margin of approximately 10 h was necessary for AC-power recovery to achieve the same magnitude of ΔCDP as the dynamic PRA. It is necessary to perform T–H simulations that account for time-dependent uncertainties, similar to those performed in dynamic PRA, to justify this value technically under these conditions. These findings suggest that the dynamic PRA results could be used to refine the modeling of classical PRA.

The author focused on core damage timing and time-dependent RAW as helpful information obtained from dynamic PRA other than ΔCDP. The author demonstrated that the proposed method could be used to calculate how countermeasures affect core damage timing and its uncertainty. About time-dependent RAW, it was shown that it is possible to quantify the amount of increase in risk considering when it fails, not just whether it fails or not. These results show that dynamic PRA can provide detailed information that classical PRA cannot. The results are consistent with the conclusions of Coyne et al. [37], who showed that dynamic PRA improves communication between decision-makers.

The results of this study are insufficient for practical decision-making because various assumptions are employed to simplify the problem. Specifically, the author ignored initiating events other than LOOP and did not use the realistic data of the mitigation system such as failure probability and timing. In real situations, accident sequences with greater complexity, such as RCP seal LOCA and stack open of power-operated relief valve, may occur. Furthermore, this study's justification of assumptions and simplification was limited due to the lack of data sources, such as the failure time of mitigation systems. Eliminating these assumptions will allow dynamic PRA analysts to model accident scenarios more realistically and obtain risk information with a higher degree of confidence. Therefore, it is necessary to obtain statistical data, such as the failure timing of systems and components not used in classical PRA. Therefore, further studies to obtain data for dynamic PRA will add value to the practical use of advanced PRA.

Despite the limitations described above, however, this study provides much-needed information on using dynamic PRA in RIDM. The author strongly believes that this study promotes advanced PRA methodology and the future use of dynamic PRA in RIDM, regulation, and safety improvement.

Acronyms

ACC: Accumulator injection system
AFW: Auxiliary feed water system
CL: Cold leg
CST: Condensate storage tank
CV: Containment vessel

DC: Down comer
HL: Hot leg
HPI: High-pressure injection system
LPI: Low-pressure injection system
PZR: Pressurizer
RWST: Refueling water storage tank
R/B: Reactor building
SG: Steam generator.

Data Availability

The data used to support the findings of this study are included within the article.

Conflicts of Interest

The authors declare that they have no conflicts of interest.

Acknowledgments

This research was conducted using the supercomputer HPE SGI8600 in JAEA. The author is grateful to the staff of the Center for Computational Science & e-Systems of JAEA. The development of RAPID is supported financially by NRA, Japan.

References

[1] U.S. Nuclear Regulatory Commission, *Significance Determination Process, Inspection Manual Chapter 0609*, U.S. Nuclear Regulatory Commission, Washington, DC, USA, 2011.

[2] U.S. Nuclear Regulatory Commission, *Independent Verification of the Mitigating Systems Performance index (MSPI) Results for the Pilot Plants, NUREG-1816*, U.S. Nuclear Regulatory Commission, Washington, DC, USA, 2005.

[3] U.S. Nuclear Regulatory Commission, *NRC Incident Investigation Program, Management Directive 8.3*, U.S. Nuclear Regulatory Commission, Washington, DC, USA, 2001.

[4] U.S. Nuclear Regulatory Commission, *Reactor oversight process, NUREG-1649*, U.S. Nuclear Regulatory Commission, Washington, DC, USA, 2006.

[5] Nuclear Energy Institute, *Industry guideline for monitoring the effectiveness of maintenance at nuclear power plants, NUMARC 93-01, Revision 4A*, Nuclear Energy Institute, Washington, DC, USA, 2011.

[6] Nuclear Energy Institute, *Risk–informed Technical Specifications Initiative 4b, Risk–Managed Technical Specifications (RMTS) Guidelines Industry Guidance Document, NEI 06-09, Revision 0*, Nuclear Energy Institute, Washington, DC, USA, 2006.

[7] Nuclear Energy Institute, *Risk–informed technical specifications initiative 5b, risk–informed method for control of surveillance frequencies industry guidance document, NEI 04-10, Revision 1*, Nuclear Energy Institute, Washington DC, USA, 2007.

[8] N. Siu, M. Stutzke, S. Dennis, and D. Harrison, *Probabilistic Risk Assessment and Regulatory Decisionmaking: Some Frequently Asked Questions*, NUREG-2201, U.S. Nuclear Regulatory Commission, Washington, DC, USA, 2016.

[9] Nuclear Regulation Authority, *Convention on Nuclear Safety National Report of Japan for 8th Review Meeting*, Nuclear Regulation Authority, Tokyo, Japan, 2019.

[10] A. K. Verma, S. Ajit, and D. R. Karanki, *Reliability and Safety Engineering*, Springer London, Berlin, Germany, 2016.

[11] D. Mandelli, S. Prescott, C. Smith et al., "A flooding induced station blackout analysis for a pressurized water reactor using the RISMC toolkit," *Science and Technology of Nuclear Installations*, vol. 2015, Article ID 308163, 14 pages, 2015.

[12] D. Mandelli, A. Alfonsi, C. Wang et al., "Mutual integration of classical and dynamic PRA," *Nuclear Technology*, vol. 207, no. 3, pp. 363–375, 2021.

[13] Y. H. J. Chang and A. Mosleh, "Cognitive modeling and dynamic probabilistic simulation of operating crew response to complex system accidents. Part 1: overview of the IDAC Model," *Reliability Engineering & System Safety*, vol. 92, no. 8, pp. 997–1013, 2007.

[14] Y. Li and A. Mosleh, "Dynamic simulation of knowledge based reasoning of nuclear power plant operator in accident conditions: modeling and simulation foundations," *Safety Science*, vol. 119, pp. 315–329, 2019.

[15] M. Kloos and J. Peschke, "MCDET: a probabilistic dynamics method combining Monte Carlo simulation with the discrete dynamic event tree approach," *Nuclear Science and Engineering*, vol. 153, no. 2, pp. 137–156, 2006.

[16] M. Kloos and J. Peschke, "Improved modelling and assessment of the performance of firefighting means in the frame of a fire PSA," *Science and Technology of Nuclear Installations*, vol. 2015, Article ID 238723, 10 pages, 2015.

[17] A. Hakobyan, T. Aldemir, R. Denning et al., "Dynamic generation of accident progression event trees," *Nuclear Engineering and Design*, vol. 238, no. 12, pp. 3457–3467, 2008.

[18] U. Catalyurek, B. Rutt, K. Metzroth et al., "Development of a code-agnostic computational infrastructure for the dynamic generation of accident progression event trees," *Reliability Engineering & System Safety*, vol. 95, no. 3, pp. 278–294, 2010.

[19] J. M. Izquierdo, J. Hortal, M. Sanchez Perea, E. Meléndez, C. Queral, and J. Rivas-Lewicky, "Current status and applications of integrated safety assessment and simulation code system for ISA," *Nuclear Engineering and Technology*, vol. 49, no. 2, pp. 295–305, 2017.

[20] C. París, C. Queral, J. Mula et al., "Quantitative risk reduction by means of recovery strategies," *Reliability Engineering & System Safety*, vol. 182, pp. 13–32, 2019.

[21] C. Picoco, V. Rychkov, and T. Aldemir, "A framework for verifying dynamic probabilistic risk assessment models," *Reliability Engineering & System Safety*, vol. 203, Article ID 107099, 2020.

[22] L. Desgeorges, P. Y. Piriou, T. Lemattre, and H. Chraibi, "Formalism and semantics of PyCATSHOO: a simulator of distributed stochastic hybrid automata," *Reliability Engineering & System Safety*, vol. 208, Article ID 107384, 2021.

[23] S. Baek, G. Heo, T. Kim, and J. Kim, "Introduction to DICE (Dynamic Integrated Consequence Evaluation) toolbox for checking coverability of operational procedures in NPPs," in *Proceedings of the 29th European Safety and Reliability Conference (ESREL2019)*, Hannover, Germany, September 2019.

[24] G. Heo, S. Baek, D. Kwon, H. Kim, and J. Park, "Recent research towards integrated deterministic-probabilistic safety assessment in Korea," *Nuclear Engineering and Technology*, vol. 53, no. 11, pp. 3465–3473, 2021.

[25] H. G. Lim, S. H. Han, and J. J. Jeong, "MOSAIQUE - a network based software for probabilistic uncertainty analysis of

computerized simulation models," *Nuclear Engineering and Design*, vol. 241, no. 5, pp. 1776–1784, 2011.

[26] J. Cho, Y. Kim, J. Kim, J. Park, and D.-S. Kim, "Realistic estimation of human error probability through Monte Carlo thermal-hydraulic simulation," *Reliability Engineering & System Safety*, vol. 193, Article ID 106673, 2020.

[27] X. Zheng, H. Tamaki, T. Sugiyama, and Y. Maruyama, "Severe accident scenario uncertainty analysis using the dynamic event tree method," in *Proceedings of the 14th International Conference on Probabilistic Safety Assessment and Management*, Los Angeles, CA, USA, September 2018.

[28] K. Kubo, S. Jang, T. Takashi, and A. Yamaguchi, "Quasi-Monte Carlo sampling method for simulation-based dynamic probabilistic risk assessment of nuclear power plants," *Journal of Nuclear Science and Technology*, vol. 59, no. 3, pp. 357–367, 2022.

[29] X. Zheng, H. Tamaki, T. Sugiyama, and Y. Maruyama, "Dynamic probabilistic risk assessment of nuclear power plants using multi-fidelity simulations," *Reliability Engineering & System Safety*, vol. 223, Article ID 108503, 2022.

[30] M. Kajimoto, K. Muramatsu, N. Watanabe, M. Funasako, and T. Noguchi, "Development of THALES-2: a computer code for coupled thermal-hydraulics and fission product transport analyses for severe accident at LWRs and its application to analysis of fission product revaporization phenomena," in *Proceedings of the International Topical Meeting on Safety of Thermal Reactors*, USA, 1991.

[31] J. Ishikawa, K. Kawaguchi, and Y. Maruyama, "Analysis for iodine release from unit 3 of Fukushima Dai-ichi nuclear power plant with consideration of water phase iodine chemistry," *Journal of Nuclear Science and Technology*, vol. 52, pp. 308–314, 2015.

[32] X. Zheng, J. Ishikawa, T. Sugiyama, and Y. Maruyama, "Bayesian optimization analysis of containment-venting operation in a boiling water reactor severe accident," *Nuclear Engineering and Technology*, vol. 49, no. 2, pp. 434–441, 2017.

[33] H. Shiotsu, J. Ishikawa, T. Sugiyama, and Y. Maruyama, "Influence of chemical speciation in reactor cooling system on pH of suppression pool during BWR severe accident," *Journal of Nuclear Science and Technology*, vol. 55, no. 4, pp. 363–373, 2018.

[34] K. Nanjo, J. Ishikawa, T. Sugiyama, M. Pellegrini, and K. Okamoto, "Revolatilization of iodine by bubbly flow in the suppression pool during an accident," *Journal of Nuclear Science and Technology*, vol. 59, no. 11, pp. 1407–1416, 2022.

[35] K. Kubo, X. Zheng, Y. Tanaka et al., "Simulation-based dynamic probabilistic risk assessment of an internal flooding-initiated accident in nuclear power plant using THALES2 and RAPID," *Proceedings of the Institution of Mechanical Engineers, Part O: Journal of Risk and Reliability*, April 2022.

[36] K. Kubo, S. Jang, T. Takata, and A. Yamaguchi, "Dynamic probabilistic risk assessment of seismic-induced flooding in pressurized water reactor by seismic, flooding, and thermal-hydraulics simulations," *Journal of Nuclear Science and Technology*, vol. 60, no. 4, pp. 359–373, 2023.

[37] K. Coyne, C. Hunter, G. DeMoss, N. Siu, Y. Li, and A. Mosleh, "Nuclear power plant precursor risk assessment using a dynamic probabilistic risk method," in *Proceedings of the 11th International Probabilistic Safety Assessment and Management Conference and the Annual European Safety and Reliability Conference (PSAM11 and ESREL2012)*, Helsinki, Finland, January 2012.

[38] U. S. Nuclear Regulatory Commission, *Final Precursor Analysis, H. B. Robinson – Electrical Fault Caused Fire and Subsequent Reactor Trip with a Loss of Reactor Coolant Pump Seal Injection and Cooling, ADAMS ML112411359*, U. S. NRC, Washington, DC, USA, 2011.

[39] The RELAP5 Development Team, RELAP5/MOD3 Code Manual, Code Structure, System Models, and Solution Methods, NUREG/CR-5535, INEL-95/0174, vol. 5, rev. 1, U.S. Nuclear Regulatory Commission, Washington, DC, USA, 1995.

[40] N. Siu and D. Collins, "PRA research and the development of risk—informed regulation at the U.S. Nuclear Regulatory Commission," *Nuclear Engineering and Technology*, vol. 40, no. 5, pp. 349–364, 2008.

[41] H. Lee, T. Kim, and G. Heo, "Application of dynamic probabilistic safety assessment approach for accident sequence precursor analysis: case study for steam generator tube rupture," *Nuclear Engineering and Technology*, vol. 49, no. 2, pp. 306–312, 2017.

[42] Korea Institute of Nuclear Safety, *Operational Performance Information System for Nuclear Power Plant (OPIS)*, Korea Institute of Nuclear Safety, Daejeon, South Korea, 2022, https://opis.kins.re.kr/opis?act=KEOBA4300P&eventSeqn=624.

[43] J. J. Jeong, K. S. Ha, B. D. Chung, and W. J. Lee, "Development of a multi-dimensionalthermal-hydraulic system code, MARS 1.3.1," *Annals of Nuclear Energy*, vol. 26, no. 18, pp. 1611–1642, 1999.

[44] Japan Nuclear Technology Institute, *Nuclear Information Archives (NUCIA)*, Japan Nuclear Technology Institute, Japan, 2022, http://www.nucia.jp/nucia/kn/KnTroubleView.do?troubleId=9321.

[45] Japan Nuclear Energy Safety Organization, *Analysis and Assessment of Safety Information Application of Accident Precursor Analysis*, JNES/SAE08-005, Japan Nuclear Energy Safety Organization, Japan, 2009, in Japanese.

[46] The Federation of Electric Power Companies of Japan, *New Framework for Japanese Electric Industry to Enhance Reactor Safety*, The Federation of Electric Power Companies of Japan, Tokyo, Japan, 2012.

[47] Tokyo Electric Power Company Holdings, *Primary Measures for Kashiwazaki-Kariwa NPS Units 6/7 to Comply with the New Regulatory Requirements*, Tokyo Electric Power Company Holdings, Tokyo, Japan, 2017.

[48] U. S. Nuclear Regulatory Commission, PRA procedures guide NUREG/CR-2300, vol. 1, U. S. Nuclear Regulatory Commission, Washington, DC, USA, 1983.

[49] Atomic Energy Society of Japan, *A Standard of Procedures of Probabilistic Safety Assessment of Nuclear Power Plants during Power Operation (Level 1 PSA): 2008*, Atomic Energy Society of Japan, Japan, 2009, in Japanese.

[50] C. Smith, J. Knudsen, K. Kvarfordt, and T. Wood, "Key attributes of the SAPHIRE risk and reliability analysis software for risk-informed probabilistic applications," *Reliability Engineering & System Safety*, vol. 93, no. 8, pp. 1151–1164, 2008.

[51] C. Hunter, *Nuclear Regulatory Commission accident sequence precursor program summary description, Revision 1*, Vol. 1, U.S. Nuclear Regulatory Commission, Washington, DC, USA, 2020.

[52] H. E. Lambert, *Measures of Importance of Events and Cut Sets in Fault Trees, UCRL-75853*, Lawrence Livermore Laboratory, California, USA, 1974.

[53] W. E. Vesely and T. C. Davis, "Two measures of risk importance and their application," *Nuclear Technology*, vol. 68, no. 2, pp. 226–234, 1985.

[54] Z. W. Birnbaum, "On the Importance of Different Components in a Multicomponent System," in *Multivariate Analysis II*, P. R. Krishnaiah, Ed., Academic Press, New York, USA, 1969.

[55] E. Borgonovo and G. E. Apostolakis, "A new importance measure for risk-informed decision making," *Reliability Engineering & System Safety*, vol. 72, no. 2, pp. 193–212, 2001.

[56] D. Mandelli, Z. Ma, C. Parisi, A. Alfonsi, and C. Smith, "Measuring risk-importance in a dynamic PRA framework," *Annals of Nuclear Energy*, vol. 128, pp. 160–170, 2019.

[57] Z. K. Jankovsky, M. R. Denman, and T. Aldemir, "Dynamic importance measures in the ADAPT framework," *Transactions of the American Nuclear Society*, vol. 115, pp. 799–802, 2016.

[58] T. Sakurahara, S. Reihani, E. Kee, and Z. Mohaghegh, "Global importance measure methodology for integrated probabilistic risk assessment," *Proceedings of the Institution of Mechanical Engineers - Part O: Journal of Risk and Reliability*, vol. 234, no. 2, pp. 377–396, 2020.